Memoirs of the Faculty of Science, Kyoto University, Series of Physics, Astrophysics, Geophysics and Chemistry, Vol. XXXV, No. 2 and 3, Article 5, 1979

EXTINCTION MEASUREMENTS OF THE TYPICAL LARGE GLOBULES BY STAR COUNTS ON THE PALOMAR OBSERVATORY SKY SURVEY PRINTS

By

Takashi SAITO and Yoshio TOMITA

Department of Astronomy, Faculty of Science, Kyoto University, Sakyo-ku, Kyoto, 606

(*Received January 31, 1979*)

1. *Introduction*

On photographs of the Milky Way (e.g. the excellent photograph by Barnard (1927)), many dark markings against the rich star fields are seen. Especially, the opaque objects in these with angular size between ten to thirty arc minutes have been of interest as "Bok Globules", since Bok and Reilly (1947) first suggested that they are possibly unit interstellar clouds in the process of starformation. In order to investigate whether they can collapse gravitationally and starformation can really occur in them, one must estimate their masses, and internal distribution of masses.

Since radio molecular line observations have been developed rapidly in the last few years, several large globules have been observed in detail (Martin and Barrett (1978)), and their physical properties are becoming clear recently. Going with that, the study of large globules by classical star counts method is being again regarded as important to know their basic parameters mentioned above. Further, the correlation between dust and molecules is one of the interesting problems in relation to the physical state of the dust globules, especially to the molecullar formation processes, and this will be studied in more detail for each globule. For several globules, the extinctions and the dust masses are obtained on the assumption of appropriate dust grain model by Bok and McCarthy (1974), Schmidt (1975), and Dickman (1978).

From these points of view, we selected typical Bok globules and determined the distributions of extinction for each object as in detail as possible by star counts. In this paper we report the raw numbers of stars counted and the distributions of extinctions for fourteen globules obtained from the following procedure. These results are used to discuss the dynamical property of Bok globule, which is presented by Tomita et al. (1979).

2. *Method of Star Counts and Results*

We picked up the globules which have rather round shape for the simplicity of dynamical discussion. These are listed in Table 1. Counts were carried on the copies of Palomar Observatory Sky Survey (POSS) prints with magnification about ten, overlaid by square grids or concentric ring reseau. Mainly, we used POSS red prints in order to detect as many stars behind the globule as possible. The limiting magnitude of the material used is 17 mag. on red, and 21 mag. on blue POSS prints, and 15 mag. on the infrared plate which is taken by the 105/150/330 cm Schmidt

Table 1. Selected 14 large globules.

Name		Position***				
Lynds*	Barnard**	l^{II} (1950)	b^{II} (1950)	α (1950)	δ (1950)	Shape
L134		4°.11	+35°.72	$15^h50^m57^s$	− 4°34′ 2″	Elliptical
L406	B95	19.48	+ 0.29	18 22 42	−11 50 28	Round
L543	B134	29.13	− 6.19	19 3 58	− 6 15 52	Round
L548	B113	28.98	− 1.85	18 48 11	− 4 25 25	Round
L663	B335	44.93	− 6.56	19 34 36	+ 7 27 15	Round
L954		88.36	+ 0.91	20 59 42	+47 32 2	Round
L970	B361	89.36	− 0.70	21 10 40	+47 10 30	Round
L1075	B157	96.82	+ 2.17	21 31 47	+54 26 50	Round
L1407		151.34	+ 4.10	4 26 5	+54 19 31	Round
L1523		172.75	− 5.45	5 2 38	+31 49 25	Round
—	B34	176.60	+ 1.40	5 39 36	+32 32 34	Round
L1570	B227	190.69	− 0.46	6 4 30	+19 28 18	Round
L1771	B87	358.91	− 5.24	18 0 52	−32 31 5	Ring
L1780		359.13	+ 36.69	15 37 31	− 6 59 59	Elliptical

* Lynds (1962).
** Barnard (1927).
*** Each coordinate in the table are the position of globule center denoted by+sign in Figure 1 to 12.

telescope at Kiso Observatory. Method, material and number of times of counts are summerized in Table 2 for each object. The distribution of the counted number is shown by Fig. 1 to 12, where the mean number is shown for the object counted more than two times. Count error in this case is not greater than 10% in the rich star field out of the globule.

Table 2. Record of Starcounts Data of the Globules.

Name	Method of* Starcounts	Material**	Number of Counts Times	Correspondance to Figure or Table
L134	G	POSS red	1	figure 1, 13
L406	G	POSS red	1	figure 2, 14
	R	POSS red	3	table 3
L543	R	POSS red	3	table 4
L548	G	POSS red	1	figure 3, 15
L663	R	POSS red	3	table 5
L954	R	POSS red	3	table 6
L970	G	POSS blue	1	figure 4, 16
	G	POSS red	1	figure 5, 17
	G	Kiso IN	4	figure 6, 18
L1075	R	POSS red	3	table 7
L1407	G	POSS red	3	figure 7, 19
L1523	R	POSS red	3	table 8
B34	G	POSS blue	1	figure 8, 20
	G	POSS red	1	figure 9, 21
L1570	R	POSS red	1	table 9
L1771	G	POSS red	2	figure 10, 22
(center)	G	POSS red	2	figure 11, 23
L1780	G	POSS red	2	figure 12, 24

* G: grid, R: concentric ring.
** POSS red, POSS blue: Palomar Observatory Sky Survey red print, blue print, Kiso IN: near infrared sensitive plate taken by the Schmidt Telescope at Kiso Observatory.

For the object counted in concentric ring reseau, star number in each ring is converted to the number density of the stars per square degree. These star densities are displayed in Table 3 to 9 as function of distance from the globule center.

3. *Derivation of the Extinction*

Assuming following three conditions, extinction A_λ at the effective wavelength λ, where the photograph is taken, is obtained from the counted star number (or star density). That is, (1) the expected star number N_0 in the globule region if there was no extinction can be obtained by interpolating the star number outside the globule, (2) foreground stars do not significantly contribute to the counted number, and (3)

Table 3. The variations of the star density N per square minute and of the extinction values A in magnitude with the distance from the globule center are listed for L406 in which stars are counted in concentric rings. The average of the values N under the dashed line are adopted as the background star density N_0, and $N_0=$ 11.40 for this object.

r (′)	N (/□′)	A_R (mag.)
0.27	3.26	1.54
0.81	1.81	2.26
1.36	1.46	2.48
1.91	1.75	2.31
2.46	1.51	2.48
3.01	2.76	1.76
3.55	2.96	1.68
4.11	5.20	0.96
4.67	6.66	0.68
5.22	6.43	0.70
5.77	8.81	0.31
6.30	8.56	0.33
6.85	9.20	0.25
7.39	9.06	0.28
7.93	9.61	0.22
8.48	11.35	0.00
9.03	11.33	0.00
9.58	11.79	−0.04
10.10	10.91	0.05
10.63	11.42	0.00
11.19	11.57	0.00
11.73	11.42	0.00

Table 4. Same as table 3 for L543. $N_0=13.09$.

r (′)	N (/□′)	A_R (mag.)
0.21	1.85	2.18
0.61	1.97	2.11
1.01	4.59	1.21
1.41	6.22	0.88
1.81	7.70	0.64
2.21	7.71	0.64
2.61	10.78	0.26
3.01	10.90	0.23
3.41	10.64	0.26
3.79	12.28	0.09
4.18	12.12	0.09
4.59	10.16	0.32
4.99	11.65	0.14
5.39	13.24	−0.00
5.80	12.51	0.06
6.19	13.74	−0.04

Table 5. Same as table 3 for L663. $N_0=22.19$.

r (′)	N (/□′)	A_R (mag.)
0.19	0.00	4.00
0.56	0.79	3.56
0.92	3.38	2.11
1.28	8.18	1.14
1.63	10.20	0.93
1.97	13.82	0.58
2.33	17.18	0.34
2.70	18.32	0.23
3.07	19.57	0.17
3.43	23.16	−0.05
3.79	20.77	0.09
4.16	23.50	−0.08
4.52	21.36	0.06
4.87	23.04	−0.05
5.25	21.59	0.04
5.61	21.89	0.00

Table 6. Same as table 3 for L954. $N_0=10.14$.

r (′)	N (/□′)	A_R (mag.)
0.75	0.17	4.60
1.74	2.79	1.56
2.25	3.88	1.20
2.75	3.51	1.31
3.27	4.41	1.05
3.79	5.38	0.79
4.29	6.69	0.50
4.79	7.33	0.39
5.31	7.88	0.30
5.81	8.96	0.16
6.30	8.92	0.16
6.81	9.08	0.13
7.35	9.17	0.13
7.85	10.10	0.00
8.34	9.86	0.02
8.85	9.81	0.02
9.36	9.64	0.05
9.85	9.75	0.05
10.36	10.24	0.00
10.85	9.85	0.02
11.33	11.34	−0.14
11.82	10.63	−0.06

Table 7. Same as table 3 for L1075. $N_0=10.50$.

r (′)	N (/□′)	A_R (mag.)
0.19	4.26	1.11
0.58	5.58	0.81
0.96	3.24	1.46
1.35	5.08	0.92
1.72	5.10	0.89
2.10	7.98	0.37
2.48	9.73	0.10
2.88	11.43	−0.12
3.26	10.28	0.03
3.64	10.06	0.07
4.03	10.97	−0.06
4.42	10.23	0.03
4.79	10.26	0.03
5.17	10.28	0.03

Table 8. Same as table 3 for L1523. $N_0=2.57$.

r (′)	N (/□′)	A_R (mag.)
0.55	0.045	4.36
1.63	0.17	3.03
2.70	0.28	2.46
3.79	0.64	1.57
4.88	1.89	0.38
5.95	1.79	0.43
7.05	2.14	0.23
8.15	2.33	0.12
9.21	2.60	−0.00
10.24	2.48	0.06
11.34	2.69	−0.05
12.45	2.51	0.04

Table 9. Same as table 3 for L1570. $N_0=2.36$.

r (′)	N (/□′)	A_R (mag.)
0.52	0.30	2.45
1.55	0.65	1.56
2.57	2.06	0.20
3.58	1.96	0.25
4.58	1.67	0.46
5.59	2.05	0.20
6.64	2.39	0.00
7.66	2.35	0.00
8.65	2.27	0.06
9.68	2.17	0.13
10.75	2.58	−0.12
11.81	2.30	0.04
12.84	2.47	−0.06
13.83	2.40	−0.03
14.86	2.36	0.00
15.89	2.34	0.00

the gradient of the standard caliblation curve $\log \varepsilon(m)$ vs. magnitude m is not affected by color and nearly same as the Allen's (1973) data, where $\varepsilon(m)$ is the number of stars brighter than m magnitude per square degree.

On these hypothesis, somewhat unrealistic but statistically valid, we can estimate A_λ using the equation,

$$\frac{N_0}{N}=\frac{\varepsilon(m_{\rm lim}-A_\lambda)}{\varepsilon(m_{\rm lim})},$$

where $m_{\rm lim}$ shows the limiting magnitude of star counts.

The distributions of A_λ for each globule obtained in this manner are shown in

Fig. 13 to 24, and Table 3 to 9.

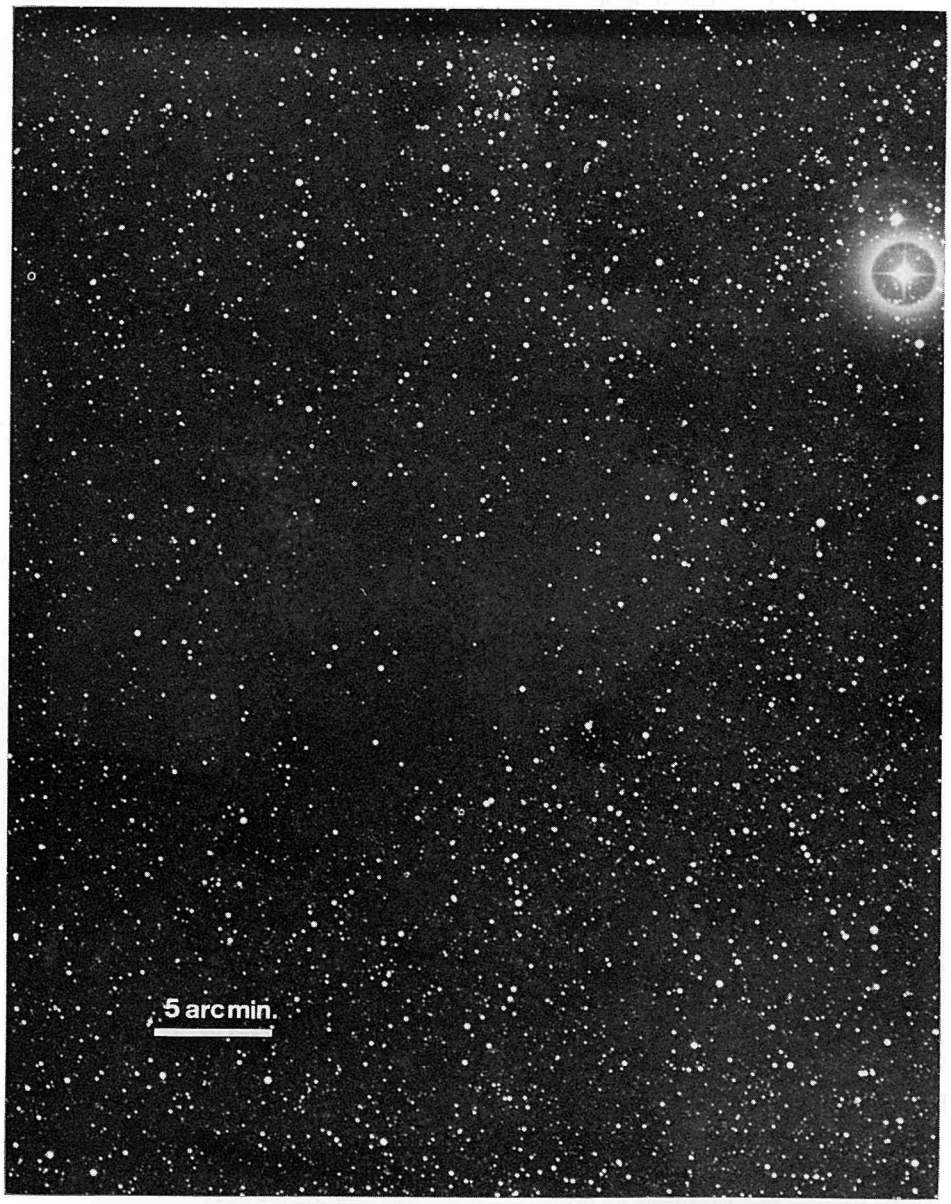

Plate. Lynds 970 is shown in this section of a photograph made with the 105/150/330 cm Schmidt telescope at Kiso Observatory, on a hyper-sensitized near infrared plate (Kodak IN emulsion bathed in ammonia solution), filter Schott RG695, exposure time 60 minutes.

Note that a few faint star images can be seen through the core of the globule. North is up and east on the left.

12	15	9	10	5	6	19	15	15	10	17
23	10	10	8	12	5	16	18	16	18	16
16	13	12	7	12	10	12	12	12	9	17
14	12	19	13	15	9	21	17	17	13	17
12	15	11	15	7	8	6	12	17	13	19
10	11	9	5	3	4	1	10	17	5	11
12	9	12	10	11	1	1	5	11	16	16
15	4	9	9	5	4	1	3	9	12	13
11	9	4	6	4	0	0	5	10	10	16
14	6	3	1	4	2	5	9	7	7	9
17	16	15	5	7	8	8	5	15	13	13
12	15	16	9	5	5	7	6	9	10	13
9	18	9	19	7	7	9	10	15	12	18
23	5	9	14	11	17	9	14	9	18	14

Fig. 1

35	41	53	45	59	53	51	57	67	69	
38	39	51	55	59	49	44	56	56	54	
47	43	37	41	35	48	41	45	42	53	
43	32	25	22	16	17	24	32	60	67	
45	31	32	14	5	5	20	46	60	76	
55	39	30	20	12	10	21	43	51	64	
73	52	29	41	12	26	27	47	58	54	
67	60	44	49	35	24	37	35	68	50	
75	70	45	43	43	47	45	44	48	62	
51	59	46	48	51	41	43	49	45	59	

Fig. 2

50	36	36	49	43	46	56	46	48	50	39	39	34	41	39	39	21	28
48	40	47	46	43	40	39	38	33	39	42	40	47	47	34	41	29	35
39	30	39	40	50	54	24	32	36	31	38	44	37	41	44	38	25	35
35	26	25	19	21	36	30	29	26	23	27	39	38	54	43	23	27	37
23	29	33	19	26	22	29	34	33	29	24	20	32	33	28	26	17	39
29	21	24	26	21	20	18	28	39	25	19	4	28	26	39	22	20	24
34	29	33	39	26	18	5	16	10	8	7	6	30	45	39	41	20	24
21	33	48	37	26	7	1	3	7	4	3	18	24	45	30	24	33	16
31	39	36	30	18	6	8	3	0	1	3	17	34	36	24	19	32	17
38	43	25	20	18	16	22	6	1	1	9	20	36	46	24	31	33	12
48	37	27	31	24	27	26	10	2	5	14	28	41	51	29	28	19	20
44	44	41	29	17	37	27	21	8	4	15	35	44	41	29	21	34	17
47	24	37	34	45	27	28	18	17	14	15	22	31	27	20	20	26	16
34	47	34	43	39	36	37	36	23	23	27	29	31	35	21	26	10	14
40	35	34	42	42	42	37	30	35	37	35	34	28	38	31	15	16	20
36	33	30	51	47	40	40	35	52	36	37	44	45	45	25	11	12	14
48	40	49	34	42	50	58	36	35	43	36	50	42	41	41	21	12	12
36	51	49	48	38	43	41	45	37	33	45	40	47	44	21	25	17	23

Fig. 3

31	36	35	24	23	14	19	23	21	31	26	34	39	25	33	29	
31	30	20	20	22	18	22	17	25	18	29	36	27	27	22	21	
38	36	23	29	23	17	29	26	20	24	14	21	14	23	14	10	
25	27	29	15	16	26	12	14	20	19	13	12	14	23	20	26	
38	33	23	20	13	10	11	11	8	19	15	19	13	27	31	27	
22	31	36	23	11	10	7	6	6	9	18	32	23	29	26	26	
31	21	26	15	13	3	1	2	3	3	4	16	27	33	36	32	
27	13	4	19	5	2	2	4	1	2	5	28	28	39	48	38	
28	22	14	16	8	8	7	6	2	0	5	21	26	36	49	49	
37	29	16	21	8	9	2	4	3	3	15	38	32	36	43	42	
38	59	33	11	10	17	4	5	11	31	47	41	36	44	48	56	
35	26	33	29	29	20	25	36	33	51	43	39	43	43	34	42	
36	31	33	35	33	33	38	36	20	37	52	37	45	36	40	53	
50	44	36	44	35	36	41	39	28	50	47	38	41	36	38	40	
45	50	36	40	43	44	33	51	41	44	33	46	33	39	36	38	
40	29	37	35	36	50	33	46	43	37	43	44	42	34	39	38	

Fig. 4

Fig. 1. Raw number of stars counted within each grids in the sky field containing L134 on the Palomar Observatory Sky Survey (POSS) red print. The grid size is $4' \times 4'$. The + sign denotes the chosen globule center listed in Table 1. The grids of which values are used to estimate the background star density N_0 are enclosed by solid lines.

Fig. 2. Same as Fig. 1 for L406 on POSS red print. The grid size is $2' \times 2'$.

Fig. 3. Same as Fig. 1 for L548 on POSS red print. The grid size is $2' \times 2'$. Since this object is surrounded by dark cloud complex, it is meaningless to get the background star density gradient from the counted data; therefore, we adopt the value 40.0 as N_0.

Fig. 4. Same as Fig. 1 for L970 on POSS blue print. The grid size is $2' \times 2'$.

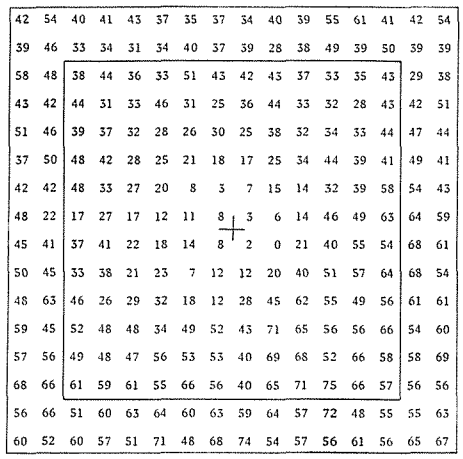

Fig. 5

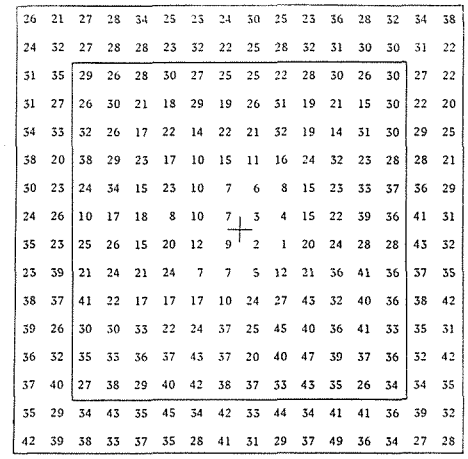

Fig. 6

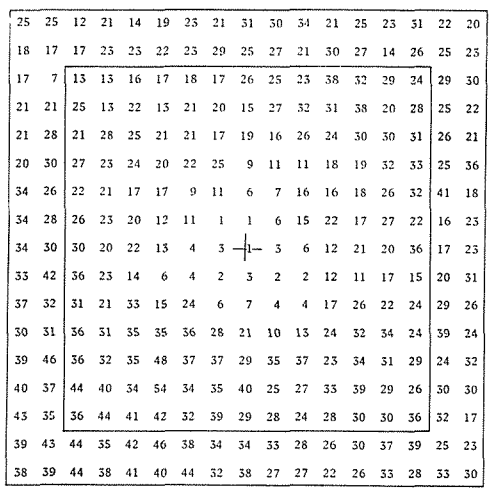

Fig. 7

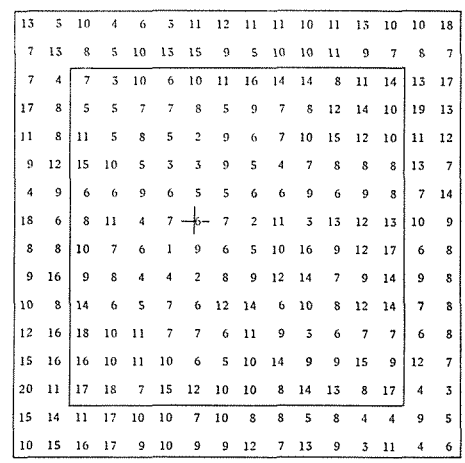

Fig. 8

Fig. 5. Same as Fig. 1 for L970 on POSS red print. The grid size is $2' \times 2'$.
Fig. 6. Same as Fig. 1 for L970 on near-infrared sensitive plate taken by the 105/150/330 cm Schmidt telescope at Kiso Observatory. The grid size is $2' \times 2'$.
Fig. 7. Same as Fig. 1 for L1407 on POSS red print. The grid size is $2'.5 \times 2'.5$.
Fig. 8. Same as Fig. 1 for B34 on POSS blue print. The grid size is $2' \times 2'$.

17	21	12	17	12	9	17	14	14	14	22	15	20	17	14	21
14	20	16	13	17	14	22	12	10	17	15	16	16	16	11	12
14	9	10	5	14	14	14	18	17	15	21	13	16	19	22	20
21	15	13	11	16	16	15	15	20	10	13	19	21	13	22	18
21	16	17	13	11	9	6	21	11	13	16	17	19	10	17	14
16	17	20	13	11	6	8	11	10	14	13	16	12	15	12	11
13	13	12	12	16	10	11	7	10	12	13	10	14	15	12	19
25	10	14	14	8	11	10	15	8	12	8	17	16	19	16	13
14	13	15	12	11	6	16	9	7	10	20	15	15	18	15	10
20	17	19	13	9	9	10	11	10	15	18	11	11	16	14	13
18	13	18	12	13	9	11	23	21	14	13	11	13	18	15	14
22	21	22	15	18	13	15	9	13	10	9	8	8	11	13	13
16	21	21	21	20	14	13	10	13	18	11	14	20	14	13	14
30	19	25	19	10	19	19	14	13	20	18	14	13	17	13	11
15	24	15	25	12	19	14	12	12	11	14	11	6	13	10	10
11	12	19	22	13	12	18	19	16	12	15	13	9	15	9	9

Fig. 9

68	73	72	68	77	79	72	71	69	65	74	73	72	75	72	71	72	78	72	74
74	76	93	81	78	71	58	75	71	63	63	81	74	84	71	67	81	79	83	78
62	72	67	66	71	73	63	65	64	67	69	68	77	67	73	68	78	74	81	84
78	66	53	65	68	70	65	78	75	61	63	59	67	73	70	72	71	85	88	84
64	65	56	88	70	75	66	66	70	71	64	74	72	80	75	79	70	75	78	76
66	75	70	84	67	61	64	77	70	70	74	82	71	85	72	69	74	70	67	73
80	77	69	69	82	74	70	75	73	80	85	83	72	82	80	74	67	70	72	78
69	62	65	67	78	81	75	76	88	78	77	80	86	72	82	76	70	71	84	75
70	64	81	78	72	82	75	76	88	84	91	87	90	86	80	74	85	73	73	87
73	65	76	81	77	76	67	76	86	98	97	99	86	85	86	83	87	90	65	75
75	70	67	74	89	72	71	79	71	86	68	69	73	82	75	84	81	75	76	81
77	82	73	86	82	92	74	80	48	46	47	73	79	79	74	90	87	75	66	75
79	72	76	77	94	91	74	65	40	52	67	63	74	82	74	92	89	78	76	70
73	70	79	76	84	82	81	38	57	54	72	57	55	74	79	80	88	73	59	77
80	69	62	90	88	78	46	48	40	55	51	49	63	78	78	86	91	86	62	77
77	67	63	65	78	90	46	54	61	61	62	44	70	71	79	80	79	69	82	76
73	63	68	75	73	76	63	64	72	53	59	70	74	73	79	79	87	65	69	77
63	68	60	75	80	72	51	80	51	60	66	74	73	63	82	91	82	81	67	71
43	66	67	55	52	47	67	74	65	60	54	77	77	71	70	75	71	66	73	76
53	54	48	46	28	51	57	81	66	67	79	72	64	70	82	75	62	79	74	81
50	65	55	45	50	56	69	73	72	59	63	74	50	56	67	66	67	66	67	73
56	66	53	52	68	65	77	65	73	66	69	66	51	46	44	54	66	64	63	66
46	47	68	70	66	81	66	76	59	63	61	56	69	44	42	61	58	62	69	48
59	63	67	67	82	72	72	62	55	66	54	42	64	48	41	47	70	65	59	47
56	71	78	61	67	84	73	61	61	54	57	56	63	42	44	42	69	67	54	34
64	78	67	68	78	62	78	69	76	73	58	60	62	62	51	60	68	57	54	49

Fig. 10

27	23	22	21	24	31	32	40	36	35	32	32	38	36	35	37
21	22	27	29	29	27	40	27	31	34	37	37	35	33	37	31
30	26	23	27	30	24	34	33	33	34	35	30	31	28	27	31
22	28	25	25	24	23	30	23	13	25	24	23	30	33	39	42
28	27	28	25	20	16	16	13	9	20	23	31	41	34	32	31
25	25	30	24	17	12	22	18	26	19	18	37	30	26	33	35
28	28	26	24	23	11	11	21	33	21	29	22	20	32	35	35
24	28	28	16	11	17	19	25	26	28	27	19	23	26	31	35
31	22	19	13	21	24	17	20	25	32	22	18	17	22	29	31
30	28	9	8	19	17	20	24	23	25	20	19	19	26	33	39
27	9	12	17	10	13	20	25	23	18	19	15	17	22	26	33
18	15	12	25	15	12	20	16	19	23	13	25	22	23	32	33
22	14	11	26	24	19	20	24	24	20	17	16	26	28	28	30
23	9	18	20	24	19	16	26	22	18	16	23	21	30	29	25
21	22	25	22	24	23	19	25	24	21	27	26	28	28	33	37
17	22	22	29	21	19	16	20	17	19	29	34	26	30	25	37

Fig. 11

13	12	20	20	20	19	23	18	15	16	16	16	26	14	13
16	18	19	16	10	13	20	20	20	16	12	17	16	16	15
19	15	15	22	21	17	13	17	24	15	10	19	18	16	15
12	24	17	19	19	19	21	13	12	14	8	14	18	21	15
16	24	14	14	21	15	12	7	17	9	9	15	20	13	18
13	20	25	17	8	12	5	11	11	12	22	19	8	21	19
16	14	12	12	7	7	8	3	4	4	11	21	20	15	18
12	26	11	11	6	8	5	5	9	5	4	19	22	14	21
18	17	16	13	4	13	19	7	9	8	8	14	15	14	12
10	17	17	15	19	12	9	9	13	8	6	17	22	17	20
18	18	17	17	17	21	12	13	16	21	13	17	21	15	12
10	18	16	20	16	11	10	15	20	21	18	19	18	14	14
20	15	18	20	15	16	20	9	16	13	17	12	15	24	13
14	13	21	19	19	15	17	20	26	16	11	16	10	12	17

Fig. 12

Fig. 9. Same as Fig. 1 for B34 on POSS red print. The grid size is $2' \times 2'$.

Fig. 10. Same as Fig. 1 for L1771 on POSS red print. The grid size is $2' \times 2'$. We adopt the mean of the star number enclosed by solid line as the value of N_0. The region enclosed by dashed line shows the detailed star counts region in Fig. 11.

Fig. 11. Same as Fig. 1 for L1771 center region on POSS red print. The grid size is $1' \times 1'$.

Fig. 12. Same as Fig. 1 for L1780 on POSS red print. The grid size is $4' \times 4'$.

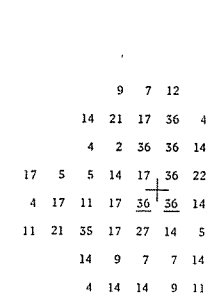

Fig. 13

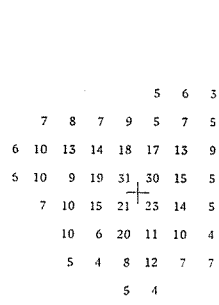

Fig. 14

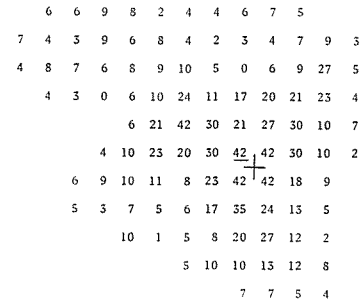

Fig. 15

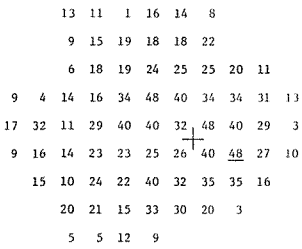

Fig. 16

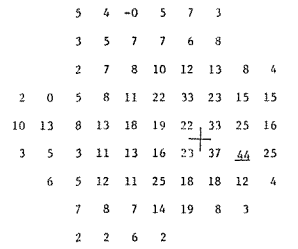

Fig. 17

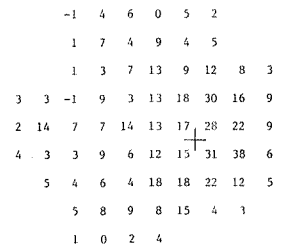

Fig. 18

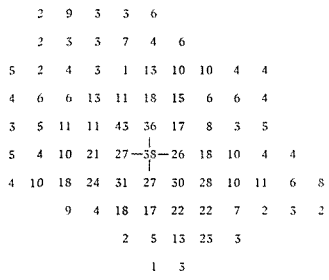

Fig. 19

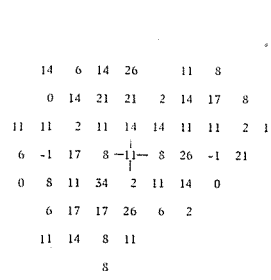

Fig. 20

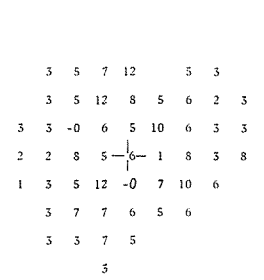

Fig. 21

Fig. 13. The extinction map at red wavelength for L134. The numerical values show the ten times of the extinction values of each grid. Underlined values show the lower limit of the extinc tion. The center of the globule is denoted by + sign.

Fig. 14. Same as Fig. 13 for L406 at red wavelength.

Fig. 15. Same as Fig. 13 for L548 at red wavelength.

Fig. 16. Same as Fig. 13 for L970 at blue wavelength.

Fig. 17. Same as Fig. 13 for L970 at red wavelength.

Fig. 18. Same as Fig. 13 for L970 at near infrared wavelength.

Fig. 19. Same as Fig. 13 for L1407 at red wavelength.

Fig. 20. Same as Fig. 13 for B34 at blue wavelength.

Fig. 21. Same as Fig. 13 for B34 at red wavelength.

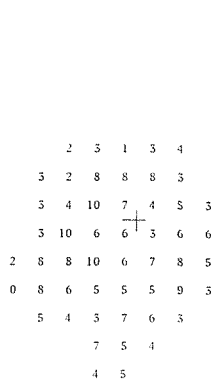

Fig. 22

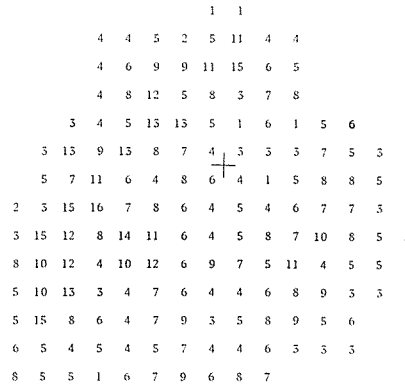

Fig. 23

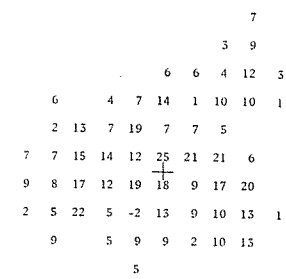

Fig. 24

Fig. 22. Same as Fig. 13 for L1771 at red wavelength.
Fig. 23. Same as Fig. 13 for L1771 center region at red wavelength.
Fig. 24. Same as Fig. 13 for L1780 at red wavelength.

REFERENCES

Allen, C. W. 1973, *Astrophysical Quantities* (Athlone Press, London), p. 243.
Barnard, E. E. 1927, *Photographic Atlas of Selected Regions of the Milky Way,* ed. Frost, E.B. and Calvert, M.R., (Carnegie Institution, Washington).
Bok, B. J. and Reilly, E. E. 1947, *Astrophys. J.*, **105**, 225.
Bok, B. J. and McCarthy, C. C. 1974, *Astrophys. J.*, **79**, 42.
Dickman, R. L. 1978, *Astron. J.*, **83**, 363.
Martin, R. N., and Barrett, A. H. 1978, *Astrophys. J. Suppl. Ser.*, **36**, 1.
Schmidt, E. G. 1975, *Monthly Notice Roy. Astron. Soc.*, **172**, 491.
Tomita, Y., Saito, T. and Ohtani, H. 1979, *Publ. Astron. Soc. Japan,* **31**, 407.